

If the experimental values of $(2H_\alpha)$ are plotted against the corresponding values of $\log a_w$, the points fall nearly on a straight line with the fit of the line well within experimental error. Least-squares analysis yields for the line

$$(2H_\alpha) = 35.3\tau - 8.17_s \log a_w \quad (3)$$

The general equation for a straight line with coordinates $(2H_\alpha)$ and $\log a_w$ is

$$(2H_\alpha) = (2H_\alpha)^0 + S \log a_w \quad (4)$$

where $(2H_\alpha)^0$ is the value of $(2H_\alpha)$ at $\log a_w = 0$, and S is the slope of the line. For any system, by definition

$$\mu_w - \mu_w^0 = 2.303 RT \log a_w \quad (5)$$

Combining Eqs. 4 and 5, we obtain Eq. 1; by substituting the values of $(2H_\alpha)^0$ and S from Eq. 3 into Eq. 1, we obtain Eq. 2.

The apparent optic axial angle $(2H_\alpha)$ depends on both $(2V_\alpha)$, the true optic axial angle of the crystal, and the refractive index of the medium in which the crystal is immersed. Thus, it is surprising that $(2H_\alpha)$, a property of the total system, should be related in such a simple manner to the chemical potential of water. Furthermore, for a system at equilibrium μ_w is everywhere the same, so that $(2H_\alpha)$ also is a measure of μ_w in the crystal.

We have also investigated a stellerite containing a small percentage of sodium ions. For this crystal the same straight-line relationship between $(2H_\alpha)$ and $\log a_w$ holds, although values of the equation constants are different.

It seems likely that Eq. 1 can be used to measure a_w in aqueous solutions either to establish thermodynamic properties or to monitor systems. Similar relationships may exist between the optic axial angle and the activity of a component in solid solutions for other systems.

G. DONALD EBERLEIN
C. L. CHRIST

U.S. Geological Survey,
Menlo Park, California 94025

References and Notes

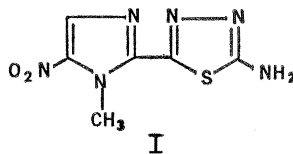
1. The optic axial angle measured in solution of known a_w is designated $(2H_\alpha)$ in contradistinction to the true optic axial angle $(2V_\alpha)$ and the apparent optic axial angle in air $(2E_\alpha)$.
2. Analysis was made by Sarah Neil, U.S. Geological Survey.
3. Analysis by G. W. Sears, Jr., U.S. Geological Survey.
4. E. W. Washburn, Ed., *International Critical Tables* (McGraw-Hill, New York, 1928), vol. 3, pp. 72-73.
5. R. A. Robinson and R. H. Stokes, *Electrolyte Solutions* (Academic Press, New York, 1959), p. 478.
6. Publication authorized by the director, U.S. Geological Survey.

14 June 1968; revised 3 October 1968

2-Amino-5-(1-methyl-5-nitro-2-imidazolyl)-1,3,4-thiadiazole: A New Antimicrobial Agent

Abstract. *The title compound has been prepared and shown to be highly active against a wide variety of gram-positive and gram-negative bacteria in mice and chicks, as well as against a number of parasitic infections in rodents.*

We have prepared a compound which we believe to be one of the most active synthetic, broad spectrum, antibacterial-antiparasitic agents known: 2-amino-5-(1-methyl-5-nitro-2-imidazolyl)-1,3,4-thiadiazole (I).



As a consequence of a program of synthesis (1) of novel nitroheterocyclic aldehydes and their elaboration into structures suggested by the antibacterial nitrofurans, structure I was prepared in 81 percent yield by the ferric ammonium sulfate oxidative cyclization of 1-methyl-5-nitroimidazole-2-carboxaldehyde thiosemicarbazone (2) in hot water. Recrystallized from dimethylformamide, the sample had a melting point of 270°-271°C; microanalysis for C, H, N, and S was satisfactory; and the nuclear magnetic resonance spectrum (dimethylsulfoxide- d_6) showed bands at τ 1.73 (singlet, ring H), τ 2.13 (broad singlet, NH_2), and τ 5.59 (singlet, CH_3).

In the chick, compound I was approximately equivalent to furazolidone orally against both *Salmonella gallinarum* and *Escherichia coli* and was highly effective against *Pasteurella multocida*. In the mouse, it was at least as effective as furazolidone orally against *Salmonella choleraesuis* and highly efficacious versus *Pasteurella multocida*. The median effective oral dose was less than 1 mg/kg against *Neisseria meningitidis* and between 10 and 90 mg/kg for *Klebsiella pneumoniae*, *Salmonella typhosa*, *Escherichia coli*, *Aerobacter aerogenes*, and *Shigella flexneri* infections in the mouse. It was highly effective against *Streptococcus pyogenes* and a number of strains of *Staphylococcus aureus*. In rodents, the agent was active against the following parasitic infections: *Trichomonas vaginalis*, *Entamoeba histolytica*, *Trypanosoma equiperdum*, *Trypanosoma cruzi*, and *Leishmania donovani*. Compound I was also active

against *Eimeria tenella* in the chick at 125 parts per million in the diet.

Test results on a large number of analogs of compound I indicate that several types of structural changes can be made, including the substitution of an aminooxadiazole for the aminothiadiazole ring, with the retention of a substantial degree of biological activity.

GERALD BERKELHAMMER
GORO ASATO

Agricultural Division,
American Cyanamid Company,
Box 400, Princeton, New Jersey 08540

References and Notes

1. G. Asato, G. Berkelhammer, E. L. Moon, *J. Med. Chem.*, in press.
2. Merck and Co., Inc., Netherlands patent 6,503,442 (1965).
3. We thank Dr. G. A. Kemp and G. S. Redin and co-workers for antibacterial data and Dr. E. J. Burden and Dr. S. Kantor and co-workers for antiparasitic data.

27 September 1968

Size-Detecting Mechanisms in Human Vision

Abstract. *Inspecting a pattern of alternating dark and light bars makes it difficult to see a similar pattern presented afterward. This phenomenon can be used to isolate mechanisms responsive to bars of a given width. Our results suggest that the human visual system contains several different classes of size detectors, each maximally sensitive to visual targets with sizes in a particular range.*

The ability to appreciate the size of an object is a basic visual perceptual function, and much research has been concerned with the indirect or higher-order processes contributing to this ability (1). We tried to determine whether, in addition to use of these indirect cues, the human visual system can directly encode the area of retinal images produced by objects of different sizes.

The observation of a pattern of alternating dark and light bars reduces the visibility of a similar pattern presented thereafter (2). This phenomenon may be exploited to isolate mechanisms responding to patterns whose bars are of a particular size. One measure of the size of a bar in a pattern of alternating light and dark bars is the number of such alternating pairs (or cycles) occupying a given area. This quantity is termed spatial frequency, with values expressed in number of cycles per degree (cycle/deg) of visual angle. In

our experiment the threshold for gratings with different spatial frequencies was measured after adaptation to gratings of various spatial frequencies. It is assumed that the ability of an adaptation pattern with a given spatial frequency to affect the visibility of a test grating with the same or some other spatial frequency reflects the extent to which the perception of both gratings depends on common mechanisms. A description of the spatial-frequency responsiveness (or tuning) of the mechanism mediating the perception of a test grating of a given spatial frequency can be obtained by an analysis of the interactions between that test grating and adaptation gratings with various spatial frequencies.

Eleven different adaptation patterns were used in our experiment. Ten were photographic square-wave gratings with horizontal bars whose spatial frequencies, at the observer's eye, were 0.18, 0.35, 0.70, 1.05, 1.40, 2.10, 2.80, 3.50, 10.12, and 22.00 cycle/deg. The luminance of a light bar of any grating was 1.35 ft lam (1 ft lam = .92 mlam); that of each dark bar was 0.45 ft lam. The 11th adaptation pattern was a uniform field whose luminance was equivalent to that of the mean luminance of the grating patterns, 0.90 ft lam. All fields were presented in Maxwellian view to the observer's right eye by a four-channel optical system (3). Each circular adaptation field subtended a visual angle of 9° and had a small, dark, central fixation point.

For the first 4 minutes of every experimental session the observer inspected one of the 11 adaptation patterns. The same pattern remained visible to the observer for the entire session except for brief periods when test grating targets were presented. To minimize the development of negative after-images of the grating bars, the adapting pattern was mechanically shifted every 3 seconds by one-half cycle, interchanging the dark and light bars. Within each session two independent determinations were made of the luminance threshold for each of three different test gratings, 0.35, 1.05, and 3.50 cycle/deg. These test gratings were oriented horizontally and appeared in the same part of the visual field as the adaptation patterns.

The following was the sequence of events on each trial. The adaptation pattern was extinguished for 0.7 second (interval 1); it reappeared for the following 1.5 seconds and was extinguished again for another period (interval 2) of 0.7 second. The adaptation

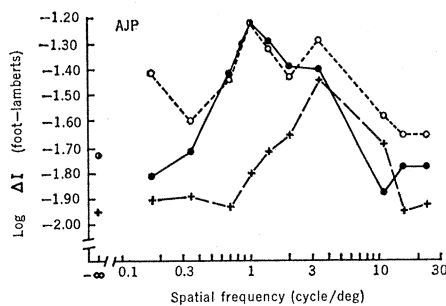


Fig. 1. Luminance threshold for test gratings of various spatial frequencies as a function of the spatial frequency of the adaptation grating. Data obtained with a test grating of 0.35 cycle/deg are indicated by unfilled circles; 1.05 cycle/deg, filled circles; and 3.50 cycle/deg, crosses. Data from observer A.P.

pattern was presented again, remaining on for the next 9.1 seconds. The entire sequence was begun again for the next trial. The test grating was presented, superposed on a homogeneous background of 0.58 ft lam, either in interval 1 or in interval 2. It occurred with equal frequency in the two intervals according to a random schedule. The interval without the test grating contained only the homogeneous background. The observer had to identify the interval containing the test grating. If this identification was wrong, the luminance of the light bars of the test grating was increased by 0.1 log unit for the presentation on the next trial. If identification was correct on three successive trials, the luminance was reduced by 0.1 log unit for the next trial. These rules for adjusting luminance to match the observer's performance generate a series of data points which bracket the stimulus value corresponding to the 79.4-percent point on the traditional "frequency of seeing" curve

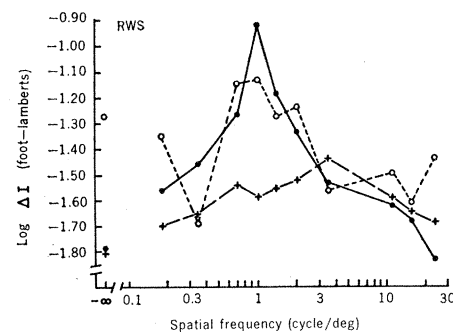


Fig. 2. Luminance thresholds for test gratings of various spatial frequencies as a function of the spatial frequency of the adaptation grating. Data obtained with a test grating of 0.35 cycle/deg are indicated by unfilled circles; 1.05 cycle/deg, filled circles; and 3.50 cycle/deg, crosses. Data from observer R.S.

(4). Each series was begun with a randomly chosen luminance for the test bars, and continued until the occurrence of five reversals in the direction of change in luminance (either decreasing to increasing, or vice versa). The threshold in a series was defined as the mean luminance of the light bars of the test grating for the last four of the five reversals in that series. Each of the two observers was tested in 22 sessions, giving four independent determinations of threshold for each of the 33 combinations of adaptation and test patterns.

Figures 1 and 2 show the mean threshold luminance of the light bars of the test target as a function of the spatial frequency of the adaptation grating. Any individual function describes the change in the threshold for a test grating of a particular spatial frequency as the spatial frequency of the adaptation grating was varied. To make statistical comparisons between the shapes of the functions, we made three separate analyses of variance. In each analysis the data obtained with a different pair of test targets were compared, and data for both observers were entered in each analysis. The analysis of variance term of interest represents the interaction between the spatial frequencies of the adaptation and test patterns. This term reflects the statistical significance of the difference between the shapes of any two test target functions.

The shape of the threshold function for the test grating of 3.5 cycle/deg differed from that obtained with test grating of 0.35 cycle/deg ($F = 3.19$, d.f. = 10,10; $P < .05$); it also differed from that obtained with the test grating of 1.05 cycle/deg ($F = 8.26$, d.f. = 10,10; $P < .01$). One obvious difference among these threshold functions is the location of their peaks. Whereas the peaks of the threshold functions for the test gratings of 0.35 and 1.05 cycle/deg occurred with the adaptation grating of 1.05 cycle/deg, the peak of the threshold function for the test grating of 3.5 cycle/deg occurred at a higher spatial frequency of the adaptation grating. This implies that the spatial-frequency tuning of the respective mechanisms is different.

In contrast to the above, the functions for the test gratings of 0.35 and 1.05 cycle/deg have nearly identical shapes ($F = 1.31$, d.f. = 10,10; $P > .25$), suggesting that the spatial-frequency tuning of the mechanisms mediating the detection of the gratings is similar. This latter finding suggests

that the number of differentially tuned classes of spatial-frequency mechanisms is limited.

These conclusions are similar to those reached by Campbell and Robson (5) from a Fourier analysis of the visibility of gratings of different spatial frequencies and waveforms. The spatial filters, identified by our method and by that of Campbell and Robson, could derive from cells in the visual system as described by Enroth-Cugell and Robson (6); each of these cells, because of the organization and size of its receptive field, tends to be maximally responsive to a grating of a particular spatial frequency.

In addition to their possible involvement in the perception of spatial extent, spatial filters may function differentially in the perception of targets moving at different speeds. Pantle (3) measured the luminance threshold for a moving test grating of constant spatial frequency presented after the observer had viewed a stationary-adaptation grating having one of a number of different spatial frequencies. Although adaptation gratings with low-spatial frequencies raised the threshold for fast-moving test gratings, adaptation gratings with high-spatial frequencies were needed to raise the threshold for slowly moving test gratings. This relation between the spatial frequency of the adaptation grating and the speed of the test grating suggests that spatial filters sensitive to large areas (low-spatial frequencies) are particularly involved in the perception of quickly moving targets; filters sensitive to small areas (high-spatial frequencies) are particular-

ly involved in the perception of slowly moving targets.

Spatial filters of the kind measured in our experiment may also contribute to the phenomenon of size constancy. When an object moves toward or away from an observer, the size of the retinal image of that object varies. The fact that phenomenal size, under a variety of conditions, remains relatively unchanged is the central fact of size constancy. Richards' (7) model of size constancy postulates shifts, during accommodation and convergence, among sets of spatial filters which, like those we have described, are tuned to different retinal image areas.

ALLAN PANTLE*

ROBERT SEKULER

Department of Psychology,
Northwestern University,
Evanston, Illinois 60201

References and Notes

1. These higher-order processes include assumptions about size, in the case of familiar objects, and judgments based on the context in which an object appears. For a discussion of these processes, see J. Hochberg, *Perception* (Prentice-Hall, New York, 1964).
 2. F. W. Campbell and J. J. Kulikowsky, *J. Physiol.* **187**, 437 (1966); K. Houlihan and R. Sekuler, *J. Exp. Psychol.* **77**, 281 (1968); R. Sekuler, *J. Exp. Psychol.* **70**, 401 (1965); R. Sekuler, E. Rubin, W. Cushman, *J. Opt. Soc. Amer.* **58**, 1146 (1968).
 3. A. Pantle, thesis, Northwestern University, Evanston, Ill. (1968).
 4. This technique is fully described, and its advantages are amplified by G. B. Wetherill and H. Levitt [*Brit. J. Math. Stat. Psychol.* **18**, 1 (1965)].
 5. F. W. Campbell and J. Robson, *J. Physiol.*, in press.
 6. C. Enroth-Cugell and J. Robson, *ibid.* **187**, 517 (1966).
 7. W. Richards, *Neuropsychologia* **5**, 63 (1967).
 8. Supported by National Institute of Neurological Diseases and Blindness grant NB-06354 to R.S.
- * Present address: Department of Psychology, University of California, Los Angeles.
- 7 August 1968; revised 17 October 1968

fibers terminating in the lateral geniculate nucleus. Since it occurs in total darkness as well as in light, it would seem to be caused by the same neural apparatus causing the eye movements. This presynaptic inhibition could provide a mechanism for a blanking of visual information during an eye movement.

My purpose was to determine whether any blanking out occurs by the time visual afferent information reaches cerebral cortical neurons. With the eye stationary, responses of single neurons in the visual cortex were studied in awake, unanesthetized monkeys and the size, shape, orientation, and location of the stationary or slowly moving visual stimulus necessary to activate the neuron (the receptive field characteristics) were determined. Then, the effect of this stimulus on the cell was tested during an eye movement.

First, rhesus monkeys were presented with a tangent screen 58 cm in front of them. Each time the monkey pressed a bar, a slit of light 0.5 degree of arc long (the fixation light) appeared at the center of the tangent screen and remained on for 1 to 3 seconds. After this variable interval, the fixation light dimmed for 400 msec; if during that time the monkey released the bar, it was rewarded with a drop of fruit juice or water. That the monkey was actually fixating during the experiment was determined by measuring the eye movements with an electrooculogram derived from the electrodes pasted on the skin.

Next, responses of spontaneously active single cells were recorded from the striate area of visual cortex by means of a movable microelectrode positioner and glass-insulated platinum microelectrodes (3). During recording, the monkey sat in a primate chair with its head held rigid (4). When single-cell activity was recorded, a search was made for its receptive field by projecting a second light (in addition to the fixation light) onto the screen. The receptive field stimulus was a white light with an intensity of 1.0 to 1.5 log units above that of the background illumination (1 cd/m²). Each time the monkey began the fixation period of several seconds, a search for the receptive field was made by moving the stimulus in the visual field and by changing its size and shape.

Finally, when the receptive field of a cell had been at least approximately determined, a horizontal, saccadic eye movement through 20 degrees of arc was elicited. The fixation light was

Visual Cortex Neurons: Response to Stimuli during Rapid Eye Movements

Abstract. While awake, unanesthetized monkeys held their eyes stationary, a motionless or slowly moving stimulus falling on the receptive field of striate cortex neurons produced an excitatory response. When a rapid eye movement was made across the same stimulus, many of these neurons continued to give an excitatory response. But the discharge of other neurons was unchanged or was suppressed during the eye movement.

With each movement of the eye, the visual world sweeps across the retina. The maximum rate of such movement during the rapid (saccadic) eye movements is about 700 degrees of arc per second for man, 900 degrees per second for monkeys (1). A stimulus moving in front of the stationary eye at this speed appears only as a blur. Yet during these

eye movements there is an apparent blanking out of vision.

During the phase of sleep characterized by rapid eye movements (2), there is a decrease in the visual evoked response in the lateral geniculate nucleus of cats with each rapid eye movement. This effect apparently results from a presynaptic inhibition of the optic tract